This paper is published in:
S.A. Krasnikov, S.I. Bozhko, K. Radican, O. Lübben, B.E. Murphy, S.-R. Vadapoo, H.-C. Wu, M. Abid, V.N. Semenov, and I.V. Shvets, *Self-Assembly and Ordering of C_{60} on the WO_2/W(110) Surface.* Nano Research **4** (2011) 194-203.

Self-Assembly and Ordering of C_{60} on the WO_2/W(110) Surface

S. A. Krasnikov[1,*], S. I. Bozhko[1, 2], K. Radican[1], O. Lübben[1], B. E. Murphy[1], S.-R. Vadapoo[1], H.-C. Wu[1], M. Abid[1, 3], V. N. Semenov[2], and I. V. Shvets[1]

[1] Centre for Research on Adaptive Nanostructures and Nanodevices (CRANN), School of Physics, Trinity College Dublin, Dublin 2, Ireland;
[2] Institute of Solid State Physics, Russian Academy of Sciences, Chernogolovka, Russian Federation;
[3] King Abdullah Institute for Nanotechnology, College of Science King Saud University, Riyadh 11451, Saudi Arabia.

Abstract

The growth and ordering of C_{60} molecules on the WO_2/W(110) surface have been studied by low-temperature scanning tunnelling microscopy and spectroscopy (STM and STS), low-energy electron diffraction (LEED) and density functional theory (DFT) calculations. The results indicate the growth of a well-ordered C_{60} layer on the WO_2/W(110) surface in which the molecules form a close-packed hexagonal structure with a unit cell parameter equal to 0.95 nm. The nucleation of the C_{60} layer starts at the substrate's inner step edges. Low-temperature STM of C_{60} molecules performed at 78 K demonstrates well-resolved molecular orbitals within individual molecules. In the C_{60} monolayer on the WO_2/W(110) surface, the molecules are aligned in one direction due to intermolecular interaction, as shown by the ordered molecular orbitals of individual C_{60}. STS data obtained from the C_{60} monolayer on the WO_2/W(110) surface are in good agreement with DFT calculations.

1. Introduction

The fabrication of complex organic molecular structures on technologically important substrates held together by weak and reversible van der Waals interactions, hydrogen bonds or electrostatic interactions has been a much investigated topic in the past ten years [1–10]. This controlled self-assembly of organic nanostructures offers a number of powerful approaches for the development of organic molecule-based devices, which possess functions such as rectifying, switching and sensing [1–8, 11–13]. Fullerenes have attracted considerable attention in recent years due to their potential in surface chemistry and nanotemplating [13], non-linear optics [13, 14], single-molecule transistors [11, 15], and especially molecular electronics because of their tunable electronic properties, resulting in superconducting or semiconducting behaviour [11, 16, 17]. The formation and characterisation of fullerene adlayers on surfaces are of great interest from the fundamental and technological points of view because they provide valuable information about molecule interactions and can lead to potential applications in existing technologies. The study of these surface-supported systems is important for future developments in molecular electronics, since they represent promising materials for applications in advanced nanopatterning, surface templating, molecular data storage, solar cells, sensors/molecular recognition and functional surfaces [11, 13–20].

[*] Author to whom any correspondence should be addressed. E-mail: krasniks@tcd.ie

Of particular interest are the nature of the bonding between the fullerene molecules and the substrate, as reflected in the electronic charge distribution and their geometric configuration at the interface, and the dynamics of electron–hole transfer between the molecule and the metal or semiconductor surface. This information can be obtained by using a combination of scanning tunnelling microscopy and spectroscopy (STM and STS). STM is a highly local technique that has become a powerful tool for studying the adsorption geometry and the conformation and dynamics of single organic molecules and molecular assemblies on conducting substrates [1–10]. Over the last decade STM has been used intensively for the study of C_{60} self-assembled layers on a variety of metal [21–36] and semiconductor [18, 37–41] surfaces. On most surfaces fullerene molecules self-assemble into close-packed monolayers with a hexagonal or quasi-hexagonal structure and a molecule–molecule separation close to 1 nm, as observed in bulk C_{60} [18, 21–25, 27–38, 41]. In some cases the formation of a C_{60} monolayer leads to an adsorbate-induced reconstruction of the substrate [22, 28, 30–36]. Surprisingly, only few studies of C_{60} on metal oxide surfaces have been performed to this end [42–44]. This is despite the fact that metal oxide surfaces and thin films have many potential applications in existing technologies [45–49] and may be used as nanostructured templates with preformed surface patterns [50–53] for molecular self-assembly.

The importance of molecule–substrate interfaces for device performance cannot be overestimated as they determine charge injection and charge flow in the molecular devices. While STM images elucidate the topographic structure of the interface, they provide little information about its electronic properties. STS is one of the best tools for probing local electronic structure with molecular spatial resolution [5, 9, 10, 25–30, 54, 55]. STS is unique in that it allows both the filled and empty state density at the surface to be probed in a single measurement, providing local density of states information close to the Fermi level. This information is vital for understanding the properties of organic molecules and their utilization in molecular electronic devices.

In the present work, by using STM/STS, LEED and DFT calculations, we focus for the first time on the molecular self-assembly of C_{60} on the WO_2/W(110) surface in the submonolayer to monolayer regimes in order to reveal the conformational behaviour of C_{60} molecules. STS and DFT are utilised to obtain information about the local density of states. The results of this work yield important information about the electronic and structural properties of C_{60} molecules adsorbed on the WO_2/W(110) surface.

2. Experimental details

The STM/STS experiments were performed at liquid nitrogen temperature (78 K), using a commercial instrument from Createc, in an ultra-high-vacuum (UHV) system consisting of an analysis chamber (with a base pressure of 2×10^{-11} mbar) and a preparation chamber (5×10^{-11} mbar). An electrochemically-etched monocrystalline W(100) tip was used to record STM images in constant current mode. The voltage V_{sample} corresponds to the sample bias with respect to the tip. No drift corrections have been applied to any of the STM images presented in this paper. Tunnelling spectra in a z(V) form were acquired on an individual C_{60} molecule. For z(V) spectroscopy, the feedback is on while the voltage ramp is applied. In this case the tip height is recorded as it approaches or retracts from the surface in order to maintain a constant tunnel current. Sudden changes in the z(V) spectra are observed when new tunnelling channels become available, or if the tip is close enough to the surface to form chemical bonds with the molecular layer or substrate. Before and after z(V) spectra acquisition, the quality of the surface was verified by STM imaging to ensure that the molecular layer remained intact and no damage was done to it during the spectroscopic measurements.

A W(110) single crystal, prepared at the Institute of Solid State Physics RAS, was used as the substrate. An atomically-clean W(110) surface was prepared by in situ annealing at 1900 K in an oxygen atmosphere of 1×10^{-7} mbar, followed by a series of high temperature flashes at 2200 K. The sample was heated by electron beam bombardment and temperatures were measured using an optical pyrometer (Ircon UX20P, emissivity 0.35). The clean W(110) surface was verified by LEED and STM before oxidation. Once a clean surface was obtained, the sample was oxidised at 1600 K in an oxygen atmosphere of 1×10^{-6} mbar for 60 minutes. The quality of the resulting oxide structure was verified by LEED and STM before the deposition of C_{60} molecules.

C_{60} (Aldrich Chemicals) was evaporated in a preparation chamber isolated from the STM chamber at a rate of about 0.2 ML (monolayer) per minute from a deposition cell operated at a temperature of approximately 700 K. Before evaporation, the C_{60} powder was degassed for about 8 h to remove water vapour. The total pressure during C_{60} deposition was in the 10^{-9} mbar range and the substrate was kept at room temperature. After deposition the sample was transferred into the STM and cooled down to 78 K for measurements.

3. Results and discussion

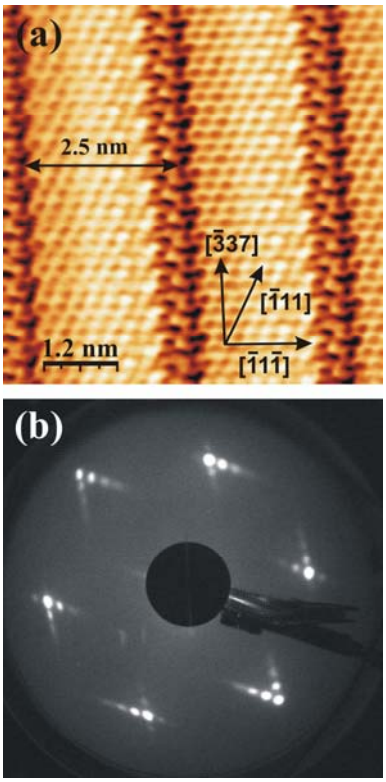

Figure 1 Low-temperature STM image of the WO_2/W(110) surface: V_{sample} = –0.06 V, I_t = 0.10 nA, size 6.5 nm × 6.5 nm, 78 K (a). LEED pattern from the WO_2/W(110) surface, acquired at a primary beam energy of 70 eV (b).

High temperature oxidation of the W(110) surface leads to the formation of an ultrathin WO_2 layer [50]. A typical STM image and a LEED pattern taken from the WO_2/W(110) surface are shown in Figs. 1a and 1b, respectively. The WO_2 has an O–W–O trilayer structure and forms well-ordered oxide nanorows on the surface, separated by 2.5 nm (Fig. 1a). These rows appear as bright regions with dark depressions in between. The LEED pattern (Fig. 1b) shows characteristic satellite spots around each primary W(110) spot, representing two equivalent overlayer domains on the surface. The WO_2 nanorows follow either the [-337] or the [-33-7] directions of the W(110) substrate depending on the domain [50]. The WO_2 overlayer has an oblique unit cell with unit cell vectors a = 2.5 nm and b = 13.0 nm, as obtained by STM and confirmed by LEED. Due to the formation of oxide nanorows, which

can influence the self-assembly of C_{60} molecules, the WO_2/W(110) surface represents an interesting nanostructured template.

At a very low coverage (0.2 ML), C_{60} molecules start nucleating at the inner step edges of the WO_2/W(110) surface (see Fig. 2a), which provides evidence for a weak molecule–substrate interaction and for the diffusion of the molecules on the surface at room temperature. C_{60} molecules appear as bright protrusions in the STM image and decorate substrate's inner step edges, forming molecular chains. The tungsten oxide nanorows of the underlying substrate are also visible (Fig. 2a). At intermediate coverage (0.4–0.7 ML), C_{60} molecules self-assemble at room temperature into compact two-dimensional islands with a hexagonal close packed structure (see Fig. 2b). The C_{60} molecular layer is incommensurate with the WO_2/W(110) substrate. However, the growth of the C_{60} overlayer starts from the substrate's inner step edges, which follow the [-111] direction on the surface. This behaviour causes one of the primary directions of the molecular layer to coincide with the [-111] direction of the WO_2/W(110) surface. This is a clear indication that the substrate plays a certain role in the adsorption and arrangement of the molecules. The angle between this direction of the C_{60} layer and the [-337] direction of the oxide nanorows is equal to 23°.

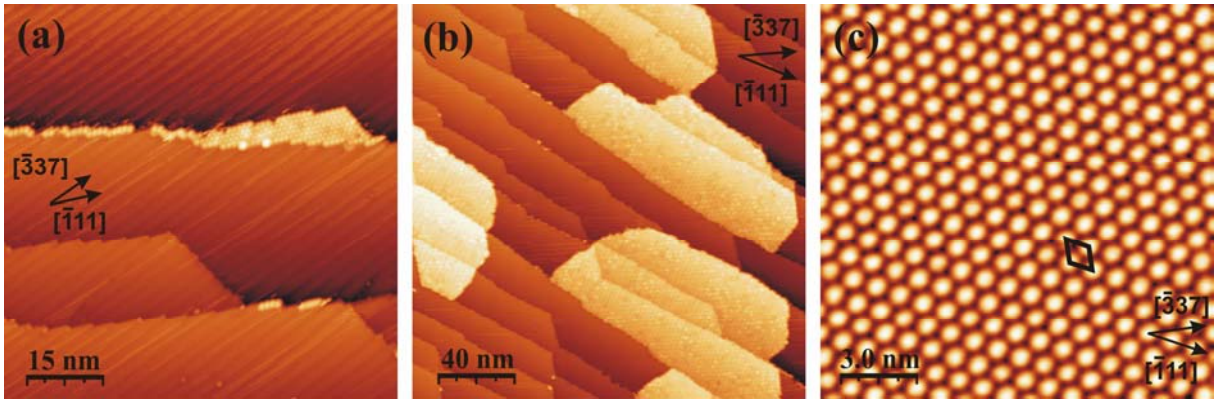

Figure 2 Low-temperature STM images acquired after the deposition of 0.2 ML (a), 0.5 ML (b) and 1 ML (c) of C_{60} molecules onto the WO_2/W(110) surface. (a) V_{sample} = +1.0 V, I_t = 0.10 nA, size 76 nm × 76 nm, 78 K. (b) V_{sample} = +1.0 V, I_t = 0.10 nA, size 200 nm × 200 nm, 78 K. (c) V_{sample} = –1.5 V, I_t = 0.13 nA, size 15.4 nm × 15.4 nm, 78 K. The unit cell of the C_{60} lattice is shown in black (c) and has the following parameters: the unit cell vectors are each equal to 0.95 nm ± 0.05 nm, and the angle between them is 60º ± 0.5º.

The intermolecular bonding that occurs through the C_{60} π-electron system (π–π stacking) appears to be stronger than the molecule–substrate interaction, leading to the formation of such compact islands. This is confirmed by the fact that there are no single C_{60} molecules adsorbed in the middle of substrate terraces after deposition, indicating a high mobility of the individual molecules on the surface at room temperature. Furthermore, each WO_2/W(110) substrate terrace is covered with a single molecular domain, with terrace widths of up to 40 nm, and domain boundaries are rarely observed. The distribution of the C_{60} among the substrate terraces is not homogeneous at this coverage - some terraces have almost no C_{60}. This indicates that C_{60} molecules can easily cross substrate step edges while moving on the surface as a result of interterrace diffusion.

At approximately 1 ML coverage, the molecules form large domains whose width is limited only by the width of the WO_2/W(110) substrate terraces. One molecular monolayer is defined as the case in which the substrate is completely covered by C_{60} molecules such that if one further molecule is added, it will have no direct contact with the substrate and will form a second layer. For the C_{60} monolayer on the WO_2/W(110) surface, the molecular packing density is 1.25 C_{60} molecules per 1 nm^2. The unit cell of the C_{60} lattice (shown in black in Fig. 2c) contains a single C_{60} molecule and has the following parameters: the unit cell vectors

are each equal to 0.95 nm ± 0.05 nm, and the angle between them is 60° ± 0.5°, forming a hexagonal close packed structure. The intermolecular separation within the overlayer is very close to the natural molecule–molecule distance of 1 nm observed in bulk C_{60} crystals. The formation of ordered domains of such an extent and the C_{60}–C_{60} separation further indicate the presence of a significant intermolecular interaction, as well as a low diffusion barrier for the molecules on the WO_2/W(110) surface at room temperature. Thus, C_{60} molecules are physisorbed on this surface and a weak molecule–substrate interaction occurs through the molecular π-electron system.

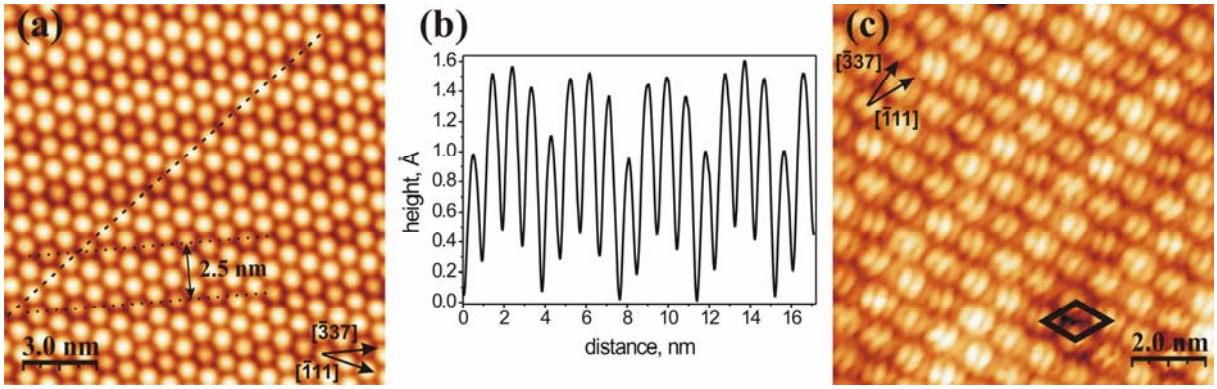

Figure 3 Low-temperature STM image of C_{60} on the WO_2/W(110) surface, showing chains of the 'dim' molecules, which occupy the grooves between the oxide nanorows of the WO_2/W(110) surface: V_{sample} = –0.7 V, I_t = 0.3 nA, size 15.6 nm × 15.6 nm, 78 K (a). Dotted lines indicate the [-337] direction of the nanorows. A line profile (along the dashed line in Fig. 3a) indicating the height difference between the 'bright' and 'dim' C_{60} (b). Low-temperature STM image of C_{60} on the WO_2/W(110) surface, showing that the C_{60} molecules are oriented in one direction at 78 K: V_{sample} = +0.9 V, I_t = 0.70 nA, size 10 nm × 10 nm, 78 K (c). The unit cell of the C_{60} overlayer is shown in black.

At some voltage biases, the C_{60} molecules on the WO_2/W(110) surface show a significant difference in apparent height (see Fig. 3a), which can be a reflection of local electronic and/or topographic variations. These so called 'bright' and 'dim' molecules have been previously observed by STM on a variety of surfaces and attributed to C_{60}-induced substrate reconstructions [22, 28, 30–36]. Such surface reconstructions can lead to two topographically different C_{60} adsorption sites, where 'dim' C_{60} molecules are sunk into nanopits of the reconstructed substrate, and are lower in height than 'bright' ones. Other explanations suggest that this apparent height difference is due to electronic and molecular orientation effects [56, 57]. From Fig. 3a it is clearly seen that the 'dim' C_{60} molecules on the WO_2/W(110) are arranged in dark chain-like structures. The distance between these chains is equal to 2.5 nm, as observed by STM. From STM images it is clear that the 'dim' C_{60} molecules follow the oxide nanorows of the substrate and are adsorbed between them. The nanostructured WO_2/W(110) surface exhibits grooves separated by 2.5 nm [50], which are seen as dark depressions in the STM image (Fig. 1a). The 'dim' C_{60} molecules observed in Fig. 3a occupy these grooves, and are situated slightly lower than the others ('bright' C_{60}). The line profile shown in Fig. 3b indicates that the height difference between the 'bright' and 'dim' C_{60} molecules is equal to approximately 0.6 Å. The same value of corrugation was observed for oxide nanorows forming the WO_2/W(110) surface [50], indicating that such an apparent height difference between C_{60} molecules is due to the substrate topography. Furthermore, the similar apparent height difference (in the range 0.4–1.0 Å) has been observed between the 'bright' and 'dim' C_{60} molecules on other surfaces and was explained by an adsorbate-induced reconstruction of the substrate [22, 28, 32–34]. However, there is also a possibility of a slightly different interaction between the WO_2/W(110) surface and the

electron orbitals of the 'dim' C_{60} molecules, caused by their specific arrangement on the surface, which results in proximity of the molecule to the W layer.

Low-temperature STM of C_{60} molecules performed at 78 K demonstrates well-resolved molecular orbitals within individual molecules. It was not possible to resolve these orbitals by performing STM at room temperature. This is most likely due to movement (rotation) of the molecules within the layer at this temperature. At 78 K however, most of the molecules in the complete C_{60} monolayer on the WO_2/W(110) surface are aligned in one direction due to the molecule–substrate interaction and the suppressed movement of the molecules at such a low temperature. This is shown in Fig. 3c by the ordered molecular orbitals (lobes) of individual C_{60}. The molecules appear on the STM image as spheres composed of three 'stripes' (molecular lobes), suggesting that the same part of each C_{60} molecule is facing the substrate. The parallel orientation of the C_{60} on the WO_2/W(110) surface indicates that the molecule–substrate interaction is strong enough to align the molecules at low temperature, when their movement is suppressed. Similar parallel orientation of the C_{60} molecules has been previously observed on certain other surfaces by low-temperature STM [25, 26, 28, 32, 33]. It is noted that STM images exhibiting three molecular lobes within an individual C_{60} molecule have been acquired at a sample bias in the range from +0.7 V to +1.0 V (+0.9 V in Fig. 3c). At such a voltage, electron tunnelling occurs into the lowest unoccupied molecular orbital (LUMO) of C_{60} (which will be shown later by STS analysis), making the LUMO responsible for the 'three-stripe' appearance of C_{60} molecules on the WO_2/W(110) surface. C_{60} molecules exhibiting three 'stripes' have been previously observed by STM on different metal and semiconductor surfaces [22, 30, 31, 40, 58, 59]. In most of these cases the proposed C_{60} orientation was the one in which the carbon–carbon bond that forms the border between two adjacent hexagons of C_{60} is parallel to the substrate [30, 31, 40, 58, 59].

In order to define the orientation of C_{60} molecules on the WO_2/W(110) surface, the ab initio density of states (DOS) calculations were performed using the Vienna Ab initio Simulation Package (VASP) program. VASP implements a projected augmented basis set (PAW) [60] and periodic boundary conditions. The electron exchange and correlation was simulated by local density approximation (LDA) pseudopotentials with a Ceperley–Alder exchange-correlation density functional [61]. A Γ-centred (2 × 2 × 1) k-point grid was used for all calculations to sample the Brillouin zone. The applied energy cut-off was 400 eV. For the DOS a smearing of 0.2 eV was applied using the Methfessel–Paxton method [62]. The global break condition for the electronic self-consistent loops was set to a total energy change of less than 1×10^{-4} eV. To find the optimum surface site of a single C_{60} molecule on one O–W–O layer of WO_2, five different surface sites were sampled and the total energy of those systems was calculated. To minimize the energy of the system, different orientations of C_{60} on the surface were simulated. For all orientations the C_{60} molecule was allowed to relax on a constrained layer of WO_2. The partial charge density of these systems was calculated in a range from E_f to 1 eV, where E_f is the Fermi energy. This partial charge density was then compared with the experimental STM images.

The molecular orientation in which the carbon–carbon bond that forms the border between two adjacent hexagons of C_{60} is parallel to the WO_2/W(110) surface (h–h orientation) was found to have the lowest energy of all other orientations under consideration. The proposed model for the C_{60} overlayer on the WO_2/W(110) surface is shown in Fig. 4. The partial charge density of the h–h orientation indicates three distinct 'stripes' as the inner structure of the C_{60} molecule (see Fig. 4, inset). This simulated inner structure is in good agreement with the lobe-resolved experimental STM images of C_{60}, suggesting that the h–h orientation is the most energetically favourable orientation of the C_{60} molecule on the WO_2/W(110) surface at 78 K.

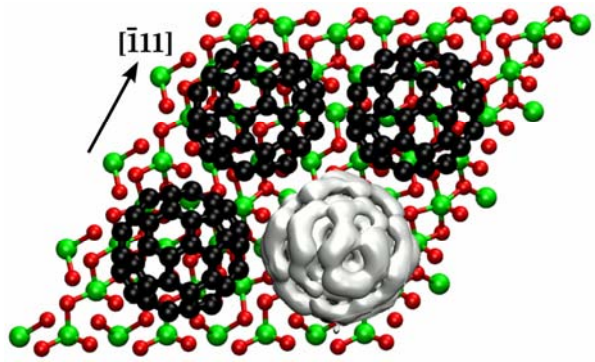

Figure 4 Schematic representation of the C_{60} overlayer on the WO_2/W(110) surface. The C atoms of C_{60} are denoted by black spheres; the O and the W atoms of the oxide layer are denoted by red and green spheres, respectively. The inset shows the partial charge density of the individual C_{60} with the h–h orientation on the surface.

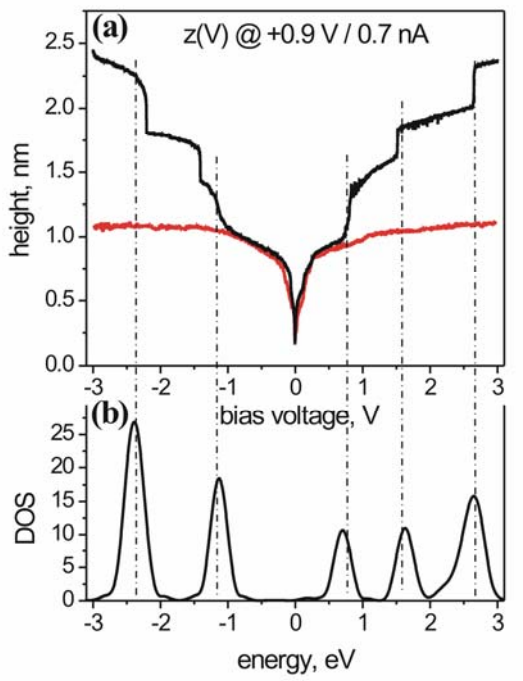

Figure 5 z(V) spectra recorded at 78 K from 1 ML of C_{60} on the WO_2/W(110) surface (black curve) and from the clean WO_2/W(110) surface (red curve) (a). The calculated DOS for the C_{60} in the h–h orientation on the WO_2/W(110) surface (b).

Figure 5 shows a comparison between the z(V) spectrum recorded at a temperature of 78 K from the C_{60} overlayer on the WO_2/W(110) surface and the result of DFT calculations for the h–h orientation of C_{60}. It is important to note that z(V) spectroscopy is an STM-based technique providing information on the density of states of the material, which is probed as a function of voltage (sample bias) through changes in the tip height [5, 9]. The z(V) spectrum was recorded at 78 K over an individual C_{60} molecule within the image shown in Fig. 3c and provides averaged information about electronic structure of the molecule. The spectrum in Fig. 5a shows five prominent features: the two steps observed at –2.3 V and –1.2 V and the three steps observed at +0.7 V, +1.6 V and +2.7 V are related to occupied and unoccupied states, respectively. These characteristic steps are seen due to the increasing number of new channels (molecular orbitals) available for tunnelling as the bias voltage increases. These features are absent on the z(V) curve obtained from the clean WO_2/W(110) surface, which proves that they are associated with the C_{60}. Furthermore, the z(V) spectrum in Fig. 5a shows good correlation with the density of states (DOS) obtained by DFT calculation (Fig. 5b). For the C_{60} on the WO_2/W(110) surface, the LUMO is located at +0.7 eV and the highest occupied molecular orbital (HOMO) at –1.2 eV. It is noted that the C_{60} molecules exhibit three distinct ‘stripes’ (molecular lobes) on STM images, when electron tunnelling occurs into the LUMO (see Fig. 3c). The HOMO–LUMO band gap of the C_{60} on the WO_2/W(110) surface obtained from STS data is equal to 1.9 eV, which is in excellent agreement with previous STS measurements of C_{60} on surfaces with low reactivity [25–30, 54, 55] and theoretical calculations [54, 55, 63, 64].

4. Conclusions

The self-assembly of C_{60} molecules on the WO_2/W(110) surface has been investigated by low-temperature STM/STS, LEED and DFT calculations. A well-ordered molecular layer was obtained in which the C_{60} molecules form a close-packed hexagonal structure with a unit cell parameter equal to 0.95 nm. The nucleation of the C_{60} layer starts at the substrate's inner step edges. Low-temperature STM of C_{60} molecules performed at 78 K demonstrates well-resolved molecular orbitals within individual molecules. Within the C_{60} monolayer on the WO_2/W(110) substrate at a temperature of 78 K, the molecules have the h–h orientation on the surface and are aligned in one direction due to intermolecular interaction, as shown by the ordered molecular orbitals of individual C_{60}. STS data obtained from the C_{60} monolayer on the WO_2/W(110) surface are in good agreement with DFT calculations. By using the WO_2/W(110) surface as a preformed nanostructured template, it was shown that the 'dim' C_{60} molecules follow the oxide nanorows of the substrate, occupy the grooves between them, and, as a result, are situated slightly lower than the others ('bright' C_{60}).

Acknowledgements
This work was supported by Science Foundation Ireland (Principal Investigator grant number 00/PI.1/C042 and Walton Visitor Award grant number 08/W.1/B2583) and by Program of Presidium of Russian Academy of Sciences. STM topographic images were processed using WSxM software [65].

References

[1] Barth, J. V. *Ann. Rev. Phys. Chem.* **2007**, *58*, 375–407.
[2] Barth, J. V.; Costantini, G.; Kern, K. *Nature* **2005**, *437*, 671–679.
[3] Barlow, S. M.; Raval, R. *Surf. Sci. Rep.* **2003**, *50*, 201–341.
[4] Rosei, F.; Schunack, M.; Naitoh, Y.; Jiang, P.; Gourdon, A.; Lægsgaard, E.; Stensgaard, I.; Joachim, C.; Besenbacher, F. *Prog. Surf. Sci.* **2003**, *71*, 95–146.
[5] Krasnikov, S. A.; Sergeeva, N. N.; Sergeeva, Y. N.; Senge, M. O.; Cafolla, A. A. *Phys. Chem. Chem. Phys.* **2010**, *12*, 6666–6671.
[6] Schnadt, J.; Xu, W.; Vang, R. T.; Knudsen, J.; Li, Z.; Lægsgaard, E.; Besenbacher, F. *Nano Res.* **2010**, *3*, 459–471.
[7] Krasnikov, S. A.; Beggan, J. P.; Sergeeva, N. N.; Senge, M. O.; Cafolla, A. A. *Nanotechnology* **2009**, *20*, 135301.
[8] Liang, H.; He, Y.; Ye, Y. C.; Xu, X. G.; Cheng, F.; Sun, W.; Shao, X.; Wang, Y. F.; Li, J. L.; Wu, K. *Coord. Chem. Rev.* **2009**, *253*, 2959–2979.
[9] Beggan, J. P.; Krasnikov, S. A.; Sergeeva, N. N.; Senge, M. O.; Cafolla, A. A. *J. Phys.: Condens. Matter* **2008**, *20*, 015003.
[10] Krasnikov, S. A.; Hanson, C. J.; Brougham, D. F.; Cafolla, A. A. *J. Phys.: Condens. Matter* **2007**, *19*, 446005.
[11] van der Molen, S. J.; Liljeroth, P. *J. Phys.: Condens. Matter* **2010**, *22*, 133001.
[12] Fichou, D. *J. Mater. Chem.* **2000**, *10*, 571–588.
[13] Bonifazi, D.; Enger, O.; Diederich, F. *Chem. Soc. Rev.* **2007**, *36*, 390–414.
[14] Xenogiannopoulou, E.; Medved, M.; Iliopoulos, K.; Couris, S.; Papadopoulos, M. G.; Bonifazi, D.; Sooambar, C.; Mateo-Alonso, A.; Prato, M. *ChemPhysChem* **2007**, *8*, 1056–1064.
[15] Park, H.; Park, J.; Lim, A. K. L.; Anderson, E. H.; Alivisatos, A. P.; McEuen, P. L. *Nature* **2000**, *407*, 57–60.
[16] Hebard, A. F.; Rosseinsky, M. J.; Haddon, R. C.; Murphy, D. W.; Glarum, S. H.; Palstra, T. T. M.; Ramirez, A. P.; Kortan, A. R. *Nature* **1991**, *350*, 600–601.
[17] Tanigaki, K.; Ebbesen, T. W.; Saito, S.; Mizuki, J.; Tsai, J. S.; Kubo, Y.; Kuroshima, S. *Nature* **1991**, *352*, 222–223.

[18] Nakaya, M.; Tsukamoto, S.; Kuwahara, Y.; Aono, M.; Nakayama, T. *Adv. Mater.* **2010**, *22*, 1622–1625.
[19] Joachim, C.; Gimzewski, J. K.; Aviram, A. *Nature* **2000**, *408*, 541–548.
[20] Hiorns, R.C.; Cloutet, E.; Ibarboure, E.; Vignau, L.; Lemaitre, N.; Guillerez, S.; Absalon, C.; Cramail, H. *Macromolecules* **2009**, *42*, 3549–3558.
[21] Zhang, X.; Tang, L.; Guo, Q. *J. Phys. Chem. C* **2010**, *114*, 6433–6439.
[22] Gardener, J. A.; Briggs, G. A. D.; Castell, M. R. *Phys. Rev. B* **2009**, *80*, 235434.
[23] Diaconescu, B.; Yang, T.; Berber, S.; Jazdzyk, M.; Miller, G. P.; Tománek, D.; Pohl, K. *Phys. Rev. Lett.* **2009**, *102*, 056102.
[24] Li, H. I.; Franke, K. J.; Pascual, J. I.; Bruch, L. W.; Diehl, R. D. *Phys. Rev. B* **2009**, *80*, 085415.
[25] Grobis, M.; Yamachika, R.; Wachowiak, A.; Lu, X.; Crommie, M. F. *Phys. Rev. B* **2009**, *80*, 073410.
[26] Zhang, X.; He, W.; Zhao, A.; Li, H.; Chen, L.; Pai, W. W.; Hou, J.; Loy, M. M. T.; Yang, J.; Xiao, X. *Phys. Rev. B* **2007**, *75*, 235444.
[27] Rogero, C.; Pascual, J. I.; Gómez-Herrero, J., Baró, A. M. *J. Chem. Phys.* **2002**, *116*, 832–836.
[28] Grobis, M.; Lu, X.; Crommie, M. F. *Phys. Rev. B* **2002**, *66*, 161408.
[29] Schulze, G.; Franke, K. J.; Pascual, J. I. *New J. Phys.* **2008**, *10*, 065005.
[30] Schull, G.; Néel, N.; Becker, M.; Kröger, J.; Berndt, R. *New J. Phys.* **2008**, *10*, 065012.
[31] Schull, G.; Berndt, R. *Phys. Rev. Lett.* **2007**, *99*, 226105.
[32] Pai, W. W.; Hsu, C.-L.; Lin, M. C.; Lin, K. C.; Tang, T. B. *Phys. Rev. B* **2004**, *69*, 125405.
[33] Abel, M.; Dmitriev, A.; Fasel, R.; Lin, N.; Barth, J. V.; Kern, K. *Phys. Rev. B* **2003**, *67*, 245407.
[34] Hsu, C.-L.; Pai, W. W. *Phys. Rev. B* **2003**, *68*, 245414.
[35] Weckesser, J.; Cepek, C.; Fasel, R.; Barth, J. V.; Baumberger, F.; Greber, T.; Kern, K. *J. Chem. Phys.* **2001**, *115*, 9001–9009.
[36] Murray, P. W.; Pedersen, M. Ø.; Lægsgaard, E.; Stensgaard, I.; Besenbacher, F. *Phys. Rev. B* **1997**, *55*, 9360.
[37] Li, Y. Z.; Patrin, J. C.; Chander, M.; Weaver, J. H.; Chibante, L. P. F.; Smalley, R. E. *Science* **1991**, *252*, 547–548.
[38] Li, Y. Z.; Chander, M.; Patrin, J. C.; Weaver, J. H.; Chibante, L. P. F.; Smalley, R. E. *Science* **1991**, *253*, 429–433.
[39] Hou, J. G.; Yang, J. L.; Wang, H. Q.; Li, Q. X.; Zeng, C. G.; Lin, H.; Bing, W.; Chen, D. M.; Zhu, Q. S. *Phys. Rev. Lett.* **1999**, *83*, 3001–3004.
[40] Pascual, J. I.; Gómez-Herrero, J.; Rogero, C.; Baró, A. M.; Sánchez-Portal, D.; Artacho, E.; Ordejón, P.; Soler, J. M. *Chem. Phys. Lett.* **2000**, *321*, 78–82.
[41] Dunn, A. W.; Svensson, E. D.; Dekker, C. *Surf. Sci.* **2002**, *498*, 237–243.
[42] Lu, C.; Zhu, E.; Liu, Y.; Liu, Z.; Lu, Y.; He, J.; Yu, D.; Tian, Y.; Xu, B. *J. Phys. Chem. C* **2010**, *114*, 3416–3421.
[43] Loske, F.; Bechstein, R.; Schütte, J.; Ostendorf, F.; Reichling, M.; Kühnle, A. *Nanotechnology* **2009**, *20*, 065606.
[44] Carvalho, A. J. P.; Ramalho, J. P. P. *Appl. Surf. Sci.* **2010**, *256*, 5365–5369.
[45] Nilius, N. *Surf. Sci. Rep.* **2009**, *64*, 595–659.
[46] Henrich, V. E.; Cox, P. A. *The Surface Science of Metal Oxides*; Cambridge University Press: Cambridge, 1994.
[47] Noguera, C. *Physics and Chemistry of Oxide Surfaces*; Cambridge University Press: Cambridge, 1996.
[48] Dedkov, Y. S.; Vinogradov, A. S.; Fonin, M.; König, C.; Vyalikh, D. V.; Preobrajenski,

A. B.; Krasnikov, S. A.; Kleimenov, E. Y.; Nesterov, M. A.; Rüdiger, U.; et al. *Phys. Rev. B* **2005**, *72*, 060401.
[49] Krasnikov, S. A.; Vinogradov, A. S.; Hallmeier, K.-H.; Höhne, R.; Ziese, M.; Esquinazi, P.; Chassé, T.; Szargan, R. *Mater. Sci. Eng. B* **2004**, *109*, 207–212.
[50] Radican, K.; Bozhko, S. I.; Vadapoo, S.-R.; Ulucan, S.; Wu, H.-C.; McCoy, A.; Shvets, I. V. *Surf. Sci.* **2010**, *604*, 1548–1551.
[51] Krasnikov, S. A.; Murphy, S.; Berdunov, N.; McCoy, A. P.; Radican, K.; Shvets, I. V. *Nanotechnology* **2010**, *21*, 335301.
[52] Radican, K.; Berdunov, N.; Shvets, I. V. *Phys. Rev. B* **2008**, *77*, 085417.
[53] Radican, K.; Berdunov, Manai, G.; N.; Shvets, I. V. *Phys. Rev. B* **2007**, *75*, 155434.
[54] Lu, X.; Grobis, M.; Khoo, K. H.; Louie, S. G.; Crommie, M. F. *Phys. Rev. B* **2004**, *70*, 115418.
[55] Lu, X.; Grobis, M.; Khoo, K. H.; Louie, S. G.; Crommie, M. F. *Phys. Rev. Lett.* **2003**, *90*, 096802.
[56] Giudice, E.; Magnano, E.; Rusponi, S.; Boragno, C.; Valbusa, U. *Surf. Sci.* **1998**, *405*, L561–L565.
[57] Altman, E. I.; Colton, R. J. *Phys. Rev. B* **1993**, *48*, 18244.
[58] Tsukamoto, S.; Nakayama, T.; Aono, M. *Carbon* **2007**, *45*, 1261–1266.
[59] Nakaya, M.; Kuwahara, Y.; Aono, M.; Nakayama, T. *Small* **2008**, *4*, 538–541.
[60] Kresse, G.; Furthmüller, J. *Phys. Rev. B* **1996**, *54*, 11169–11186.
[61] Ceperley, D. M.; Alder, B. J. *Phys. Rev. Lett.* **1980**, *45*, 566–569.
[62] Methfessel, M.; Paxton, A. T. *Phys. Rev. B* **1989**, *40*, 3616–3621.
[63] Sau, J. D.; Neaton, J. B.; Choi, H. J.; Louie, S. G.; Cohen, M. L. *Phys. Rev. Lett.* **2008**, *101*, 026804.
[64] Rivelino, R.; de Brito Mota, F. *Nano Lett.* **2007**, *7*, 1526–1531.
[65] Horcas, I.; Fernández, R.; Gómez-Rodriguez, J. M.; Colchero, J.; Gómez-Herrero, J.; Baro, A. M. *Rev. Sci. Instrum.* **2007**, *78*, 013705.